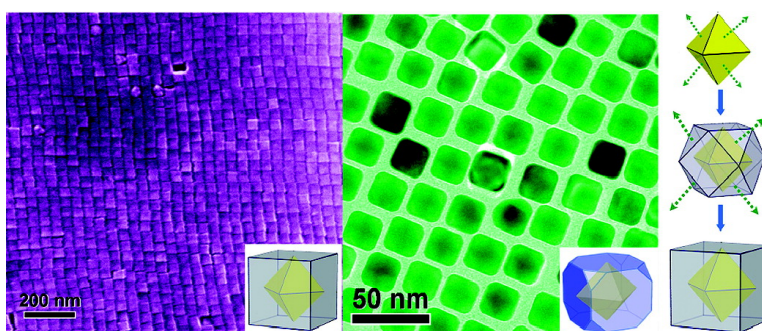# Epitaxial Growth of Heterogeneous Metal Nanocrystals: From Gold Nano-octahedra to Palladium and Silver Nanocubes

Feng-Ru Fan, De-Yu Liu, Yuan-Fei Wu, Sai Duan, Zhao-Xiong Xie, Zhi-Yuan Jiang, and Zhong-Qun Tian

More About This Article

Additional resources and features associated with this article are available within the HTML version:

- Supporting Information
- Links to the 5 articles that cite this article, as of the time of this article download
- Access to high resolution figures
- Links to articles and content related to this article
- Copyright permission to reproduce figures and/or text from this article

View the Full Text HTML

Epitaxial Growth of Heterogeneous Metal Nanocrystals: From Gold Nano-octahedra to Palladium and Silver Nanocubes

Feng-Ru Fan, De-Yu Liu, Yuan-Fei Wu, Sai Duan, Zhao-Xiong Xie,* Zhi-Yuan Jiang, and Zhong-Qun Tian*

State Key Laboratory of Physical Chemistry of Solid Surfaces and Department of Chemistry, College of Chemistry and Chemical Engineering, Xiamen University, Xiamen, China

Received March 2, 2008; E-mail: zqtian@xmu.edu.cn; zxxie@xmu.edu.cn

The construction of functional noble metal nanocrystals has received increasing interest because their unique optical, magnetic, and catalytic properties can be tuned by controlling the size, shape, chemical composition, surface and interfacial structure,[1,2] and they have potential applications such as in catalysis, biodiagnostics, plasmonics, and surface-enhanced Raman spectroscopy.[3,4] Very recently, the special attention has been paid on the shape-controlled synthesis of binary metallic heterostructures through epitaxial growth of second (third) metal over the seed metal.[5–7] As a new and very important achievement, Yang and co-workers rationally designed and used cubic Pt nanocrystals as seeds for the conformal shape-controlled epitaxial overgrowth of Pd and the anisotropic growth of Au.[8] They also showed that lattice mismatch (0.77% for Pt/Pd versus 4.08% for Pt/Au) plays a critically important role in the overgrowth of the secondary metal and high lattice mismatch prevents the conformal overgrowth. In order to extend the shape-controlled growth of binary or trinary metallic nanocrystals and get the deep insight of the growth mechanism, it is highly desirable to develop new synthesis methods and establish a general rule for epitaxial growth of heterostructured nanocrystals of a variety of metals.

In this communication, we describe a simple and effective route to synthesize bimetallic core−shell nanocubes in aqueous solution by a two-step seed-mediated growth method using Au nano-octahedra as cores. A complete conversion from octahedral metal cores into heterogeneous single-crystal nanocubes in high yield was achieved for the first time. Through a systematic investigation on the growth of core−shell heterogeneous structures of four typical noble metals (i.e., silver, gold, palladium, and platinum), we propose the relevant growth modes and more general criteria for the conformal epitaxial growth or the heterogeneous nucleation and growth of various noble metals.

As the seed-mediated growth method is a convenient and versatile synthesis method for metal nanostructures,[9] we used a modified two-step seed-mediated growth method for synthesizing Au@Pd nanocubes. Au nanoparticles of about 3 nm in diameter were first synthesized as the seeds for growing about 30 nm Au nano-octahedra as the cores. Then the uniform Au@Pd nanocubes were overgrown on the octahedral Au cores in high yield by reducing H_2PdCl_4 with ascorbic acid under the assistance of a surfactant (cetyltrimethylammonium bromide, CTAB). All the samples were characterized as prepared without any purifying. The scanning electron microscopy (SEM) and transmission electron microscopy (TEM) images show that the overall morphology of the sample and the majority of the core−shell particles adopt a perfect cubic shape with mean size of 41.5 ± 1.0 nm (Figure 1a,b). The particles tend to assemble into an ordered square array on Si substrate, indicating the highly monodispersed particles size. The STEM images and the elemental mapping of a single particle (Figure 1c)
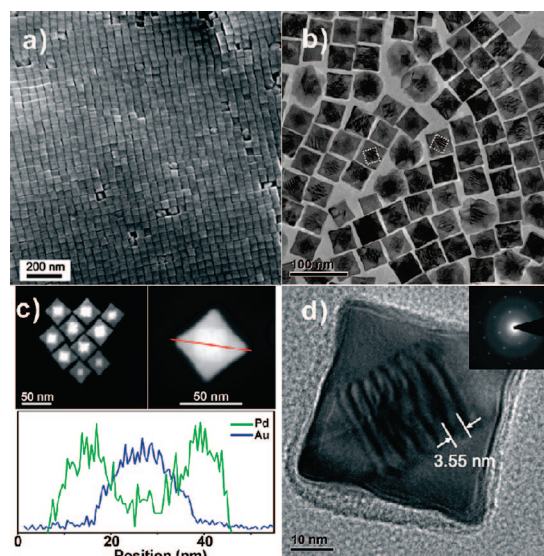

Figure 1. (a, b) SEM and TEM images of the overall morphology of Au@Pd nanocubes self-assembled on the Si wafer and Cu grid, respectively. The dashed frames indicate the core area of particles. (c) STEM images of the octahedral Au seed within a cubic Pd shell and cross-sectional compositional line profiles of a Au@Pd nanocube along the diagonal (indicated by a red line). (d) TEM image of a Au@Pd nanocube at high magnification. The inset is the SAED pattern taken from individual nanocube.

confirm the successful preparation of the core−shell structure. The selected area electron diffraction (SAED) pattern (Figure 1d) and high-resolution TEM (HRTEM) analyses (Figure S2) show that shells of the nanocubes are single-crystalline with the {100} bare surfaces.

It is of interest that the area corresponding to the Au core is completely covered with fringes formed by alternate bright and dark stripes, as shown in Figure 1b,d. These fringes are Moiré patterns due to the superposition of two misfit crystalline lattices (Pd and Au lattices).[10,11] The spacing of the Moiré fringes can be calculated for each of the different patterns using the following expression:

$$D = \frac{d_2 d_1}{d_2 - d_1}$$

where D is the spacing of two stripes and d_1 and d_2 are the misfit crystalline lattices of the overlapping planes. The spacing shown in Figure 1d is 3.55 nm, corresponding to the calculated data (3.43 nm) of the crystal lattices of Pd and Au {220} planes. As seen in the images, the Moiré fringes parallel to each other in the core area suggest that the relative orientations of both lattices are accordant and the epitaxial growth of the Pd shell occurs on the Au core.
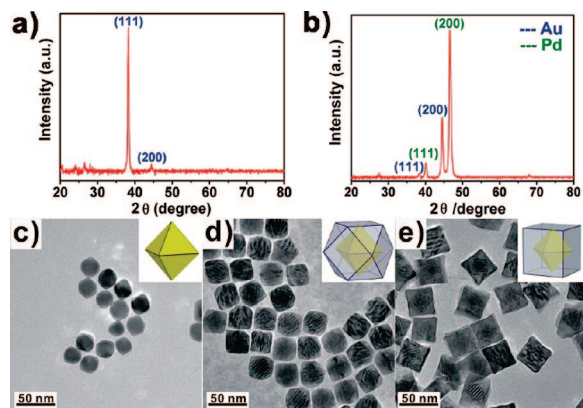
Figure 2. (a, b) Powder X-ray diffraction patterns of Au nano-octahedra and Au@Pd nanocubes, respectively. (c) The TEM image taken from Au nano-octahedral seeds. (d, e) The TEM images of Au@Pd nanoparticles prepared with 0.2 and 0.5 mL of 10 mM H_2PdCl_4 solution, respectively. The insets are models of the samples.

The X-ray diffraction (XRD) patterns recorded on Au seeds and Au@Pd nanocubes are compiled in Figure 2a,b. For Au octahedral particles, only a (111) peak clearly appears in the pattern, indicating the {111} planes of the particles have a preferential orientation (parallel to the substrate). In contrast, Au@Pd nanocubes tend to orient along {100} planes parallel to the substrate, thus giving higher (200) diffraction intensity of Pd shell than that of (111). Furthermore, they are two separate phases for Au cores and Pd shells in nanoparticles, showing that the Au cores do not affect the lattice of the epitaxial shell. Interestingly, for the Au@Pd nanocrystals, the preferential orientation of the Au seed also changes from the (111) to (100) as shown in the XRD pattern, indicating the iso-orientation between the core lattice and shell lattice. The TEM images (Figure 2c−e) taken from Au seeds and Au@Pd nanoparticles prepared with different volumes of H_2PdCl_4 show the growth pathway of the cubic Au@Pd nanocrystals. Clearly, the Au nano-octahedra first grow into truncated cubes (Figure 2d) then into cubes (Figure 2e). The decrease of the eight {111} facets of octahedral Au cores and the increase of the {100} facets of Pd shells indicates the fast growth rate along the ⟨111⟩ directions. These experimental facts suggest that the surfactant could selectively adsorb on {100} facets and lower the surfaces' energy of the {100} surface under the present experimental condition.[12]

To investigate the mechanism and rule for the epitaxial growth of heterogeneous structure of noble metals in aqueous solution, we further synthesized another two kinds of binary metal core−shell nanoparticles, Au@Ag nanocubes (Figure S3) and Au@Pt nano-spheres, in the similar reaction conditions as shown in Figure 3a−d. It can be found that Au@Ag nanoparticles exhibit uniform cubic shape and are well monodispersed. All the surfaces of the Au@Ag nanocubes are atomic smooth with no obvious defect. Figure 3a shows that each Au@Ag cube contains a dark Au core at the center and a uniform single-crystalline Ag shell. However, no obvious Moiré fringes can be observed in the core area (Figure S4) because the lattices of bulk Au and Ag have almost a perfect match (0.1%). For Au@Pt, uniform nanospheres with a rough surface were observed. The TEM image indicates that the Pt shell surrounding the octahedral Au core is polycrystalline as shown in Figure 3c and Figure S5. This dramatically different morphology suggests a three-dimensional heterogeneous nucleation and growth, rather than the layer-by-layer epitaxial growth for Pt shell on Au seeds. This result is quite surprising as the conformal epitaxial growth mode is applicable to Au@Pd nanocrystals with a large lattice mismatch
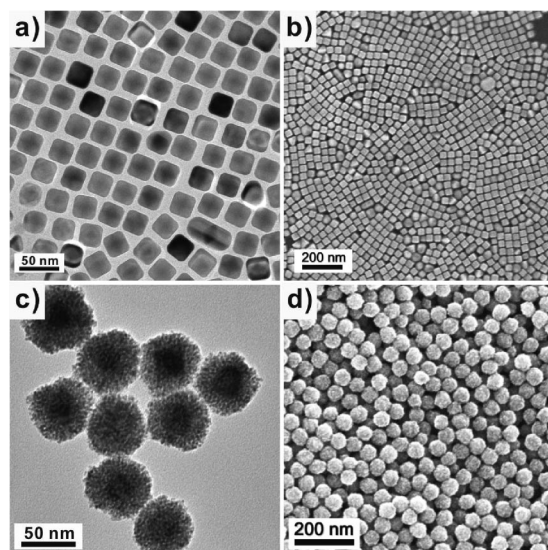

Figure 3. TEM and SEM images of (a, b) Au@Ag nanocubes and (c, d) Au@Pt nanoparticles.

(4.71%) but not to the Au@Pt one with relatively small lattice mismatch (3.80%).

It is worthwhile to clearly understand why Pd and Ag adopt epitaxial growth on Au surface but Pt does not. In addition to the lattice match, other factors and the synergetic effect of all factors to determine the growth mode must be considered. One could simply give the explanation in terms of the low surface free energy. However, this is vague especially for the growth over nanocrystals in solution with complex components consisting of second metal ions, anions, and reducing and capping agents. According to the heterogeneous nucleation and growth theory, the growth mode is mainly determined by the lattice match and interactions between the overlayer and substrate. Generally, there are three types of growth modes when a substance is deposited on a substrate in gas phase or vacuum, the layered growth (Frank−van der Merwe (F−M) mode), the island growth (Volmer−Weber (V−W) mode), and the intermediate type of growth (Stranski−Krastanow (S−K) mode).[13] According to the theory of F−M mode growth (layer-by-layer epitaxial growth mode), the metal bond energy is a key factor in addition to the lattice match. The interactions among atoms in the deposited overlayer should be smaller than that between the substrate and overlayer. Moreover, we think that the proper interaction of the overlayer and substrate, for example, the electron transfer, could be another key factor when the crystal growth occurs in solutions, which is governed by the electronegativity of two kinds of metal atoms. A good example is electrochemical underpotential deposition (UPD) in electrolyte solution.[14] The foreign metal atoms with lower electronegativity tend to wet the heterogeneous metal surface and form the two-dimensional UPD overlayer. It also prevents the galvanic displacement reaction, that is, the deposition of less active metal (with higher electronegativity) on the metal core.

Accordingly, we propose the following rules for the epitaxial layered growth of heterogeneous core−shell nanocrystals: (i) The lattice constants of two metals should be comparable with the lattice mismatch smaller than about 5%. The shell metal with smaller atom radius is easier to epitaxially grow on the core as they could uniformly release the lattice strain resulting from the lattice mismatch. (ii) The electronegativity of the shell metal is lower than the core metal in order to avoid the displacement reaction and to easily wet the surface of the core. Otherwise, the shell metal

Table 1. Comparison of Physical Constants between the Core Metal and the Shell Metal in Various Combinations of Binary Metal Nanocrystals[a]

core@shell	atomic radius r_{core} vs r_{shell}	bond dissociation energies $E_{core-core}$ vs $E_{shell-shell}$	electronegativity (Paulings) X_{core} vs X_{shell}	experimental observation of epitaxial growth
Pt@Au	small	high	low	no
Pt@Ag	small	high	high	no report
Pt@Pd	large	high	high	yes
Au@Pd	large	high	high	yes
Au@Ag	equal	high	high	yes
Au@Pt	large	low	high	no
Ag@Pd	large	high	low	no
Ag@Au	equal	low	low	no
Ag@Pt	large	low	low	no
Pd@Au	small	low	low	no
Pd@Ag	small	low	high	no report
Pd@Pt	small	low	low	no report

[a] The related physical constants of various kinds of noble metal are listed as Supporting Information.
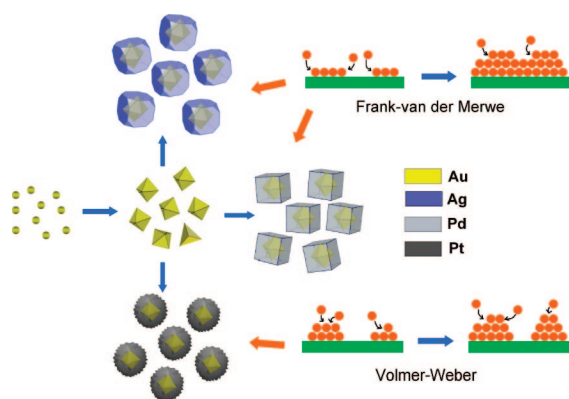
Figure 4. Schematic illustration of two typical growth modes of heterogeneous structure for binary metal core−shell nanoparticles.

intensively tends toward galvanic displacement of the core metal instead of the epitaxial growth (Figure S7).[5] (iii) The bond energy between metal atoms of the shell should be smaller than that between the shell atoms and substrate atoms in order to ensure the growth in the F−M mode. Table 1 summarizes these physical constants for four typical noble metals and the experimental observations for the layered growth mode. Only three core−shell structures (Pt@Pd, Au@Pd, and Au@Ag) can well meet the above-mentioned three rules, which is in a good agreement with our experimental result (Figures 2, 3, and S7) and the previous literature.[5,8] Further theoretical calculation on the integrative effect of the three factors above is under investigation.

In conclusion, three binary metallic core−shell nanocrystals have been successfully synthesized in high yield by a two-step seed-mediated method in a simple aqueous system. The growth of heterogeneous metal shells on the gold core presents two different forms, the conformal epitaxial growth for Au@Pd and Au@Ag nanocubes, and the heterogeneous nucleation and island growth for Au@Pt nanospheres (see Figure 4). Accordingly, we have preliminarily proposed that the atomic radius, bond dissociation energy, and electronegativity of the core and shell metals could play key roles in determining the growth mode. Moreover, the layer growth rate should be adequately low because the kinetics of the epitaxial growth could be influenced considerably by the concentration of surfactant, reducing agency, and metal ion as well as the reaction temperature. The systematic mechanistic study would be helpful

for further extending the shape-controlled epitaxial growth of core−shell nanostructure to other materials. Furthermore, the binary metal nanocubes with uniform size are easy to fabricate and process into more complex nanostructures, such as the multiple shells. The fascinating features with unique properties could become very attractive and promising building blocks for advanced materials and devices.

Supporting Information Available: Experimental details, the analysis of the production, STEM, elemental mapping, EDX and HRTEM analyses, UV−vis measurements, SEM images of Ag nanocubes and related binary metal nanostructures, and the physical constants of noble metals. This material is available free of charge via the Internet at http://pubs.acs.org.

References

(1) (a) Burda, C.; Chen, X. B.; Narayanan, R.; El-Sayed, M. A. *Chem. Rev.* **2005**, *105*, 1025. (b) Xia, Y. N.; Halas, N. J. *Mater. Res. Bull.* **2005**, *30*, 338. (c) Liz-Marzán, L. M. *Langmuir* **2006**, *22*, 32. (d) Pileni, M. P. *J. Phys. Chem. C* **2007**, *111*, 9019.

(2) (a) Wiley, B. J.; Im, S. H.; Li, Z. Y.; McLellan, J.; Siekkinen, A.; Xia, Y. N. *J. Phys. Chem. B* **2006**, *110*, 15666. (b) Murphy, C. J.; Sau, T. K.; Gole, A. M.; Orendorff, C. J.; Gao, J. X.; Gou, L. F.; Hunyadi, S. E.; Li, T. *J. Phys. Chem. B* **2005**, *109*, 13857. (c) Lee, H.; Habas, S. E.; Kweskin, S.; Butcher, D.; Somorjai, G. A.; Yang, P. D. *Angew. Chem., Int. Ed.* **2006**, *46*, 7988. (d) Bratlie, K. M.; Lee, H.; Komvopoulos, K.; Yang, P. D.; Somorjai, G. A. *Nano Lett.* **2007**, *7*, 3097.

(3) (a) Chen, M. S.; Kumar, D.; Yi, C.-W.; Goodman, D. W. *Science* **2005**, *310*, 291. (b) Rosi, N. L.; Mirkin, C. A. *Chem. Rev.* **2005**, *105*, 1547. (c) Tao, A. R.; Sinsermsuksakul, P.; Yang, P. D. *Nat. Nanotechnol.* **2007**, *2*, 435.

(4) (a) Tian, Z. Q.; Ren, B. *Annu. Rev. Phys. Chem.* **2004**, *55*, 197. (b) Orendorff, C. J.; Gole, A.; Sau, T. K.; Murphy, C. J. *Anal. Chem.* **2005**, *77*, 3261. (c) Tian, Z. Q.; Ren, B.; Li, J. F.; Yang, Z. L. *Chem. Commun.* **2007**, *34*, 3514.

(5) (a) Rodríguez-González, B.; Burrows, A.; Watanabe, M.; Kiely, C. J.; Liz-Marzán, L. M. *J. Mater. Chem.* **2007**, *15*, 1755. (b) Chen, J. Y.; Wiley, B.; McLellan, J.; Xiong, Y. J.; Li, Z. Y.; Xia, Y. N. *Nano Lett.* **2005**, *5*, 2058. (c) Camargo, P. C.; Xiong, Y. J.; Ji, L.; Zuo, J. M.; Xia, Y. N. *J. Am. Chem. Soc.* **2007**, *129*, 15452.

(6) (a) Tsuji, M.; Miyamae, N.; Lim, S.; Kimura, K.; Zhang, X.; Hikino, S.; Nishio, M. *Cryst. Growth Des.* **2006**, *6*, 1801. (b) Song, J. H.; Kim, F.; Kim, D.; Yang, P. D. *Chem.—Eur. J.* **2005**, *11*, 910. (c) Xiang, Y. J.; Wu, X. C.; Liu, D. F.; Jiang, X. Y.; Chu, W. G.; Li, Z. Y.; Ma, Y.; Zhou, W. Y.; Xie, S. S. *Nano Lett.* **2006**, *6*, 2290. (d) Xue, C.; Millstone, J. E.; Li, S. Y.; Mirkin, C. A. *Angew. Chem., Int. Ed.* **2007**, *46*, 8436.

(7) (a) Moraki, T.; Zhang, M. J.; Yang, P. *J. Am. Chem. Soc.* **2007**, *129*, 9864. (b) Yin, Y. D.; Erdonmez, C.; Aloni, S.; Alivisatos, A. P. *J. Am. Chem. Soc.* **2006**, *128*, 12671. (c) Seo, D.; Yoo, C. I.; Jung, J.; Song, H. *J. Am. Chem. Soc.* **2008**, *130*, 2940. (d) Chen, J. Y.; Wiley, B.; Li, Z. Y.; Campbell, D.; Saeki, F.; Cang, H.; Au, L.; Lee, J.; Li, X. D.; Xia, Y. N. *Adv. Mater.* **2005**, *17*, 2255.

(8) Habas, S. E.; Lee, H.; Radmilovic, V.; Somorjai, G. A.; Yang, P. D. *Nat. Mater.* **2007**, *6*, 692.

(9) (a) Nikoobakht, B.; El-Sayed, M. A. *Chem. Mater.* **2003**, *15*, 1957. (b) Sau, T. K.; Murphy, C. J. *J. Am. Chem. Soc.* **2004**, *126*, 8648. (c) Johnson, C. J.; Dujardin, E.; Davis, S. A.; Murphy, C. J.; Mann, S. *J. Mater. Chem.* **2002**, *12*, 1765.

(10) Williams, D. B.; Carter, C. B. *Transmission Electron Microscopy, a Text for Materials Science*; Plenum Press: New York, 1996.

(11) Grzelczak, M.; Rodríguez-González, B.; Pérez-Juste, J.; Liz-Marzán, L. M. *Adv. Mater.* **2007**, *19*, 2262.

(12) (a) Wang, Z. L. *J. Phys. Chem. B* **2000**, *104*, 1153. (b) Sun, Y. G.; Xia, Y. N. *Science* **2002**, *298*, 2176. (c) Kim, F.; Connor, S.; Song, H.; Kuykendall, T.; Yang, P. D. *Angew. Chem., Int. Ed.* **2004**, *43*, 3673.

(13) Bauer, E.; van der Merwe, J. H. *Phys. Rev. B* **1986**, *33*, 3657.

(14) Kolb, D. M. In *Advances in Electrochemistry and Electrochemical Engineering*; Gerisher, H., Tobias, C. W., Eds.; Wiley-Interscience: New York, 1978; Vol. 11, pp 125−271.

JA801566D